# DEVELOPMENT OF CIRCULARLY POLARIZED SYNTHETIC APERTURE RADAR ONBOARD MICROSATELLITE

**Chiba University・○J. T. Sri Sumantyo, Nihon University・H. Wakabayashi, Tokyo University・A. Iwasaki, JAXA・F. Takahashi, Sentencia Corporation・H. Ohmae, NIES・H. Watanabe, Chiba University・R. Tateishi, Chiba University・F. Nishio, Chiba University・M. Baharuddin, and Chiba University・P. Rizki Akbar**

## ABSTRACT

Previously, several types of synthetic aperture radar (SAR) sensor have been developed for many applications. These sensors work in linear polarization, high power, bulky system, and sensitive to Faraday rotation effect. To solve these problems, recently, we are developing a new type of microsatellite onboard synthetic aperture radar sensor called Circularly Polarized Synthetic Aperture Radar (CP-SAR) to improve the quality of conventional type of SAR images. The interest in the earth observation technologies is expected to increase with the CP-SAR in the coming years. In this paper, the specification of CP-SAR system is discussed.

## I. INTRODUCTION

Synthetic Aperture Radar (SAR) is a multi purpose sensor that can be operated in all-weather and day-night time. Recently, the SAR sensor is operated in linear polarization (HH, VV and its combination) [1] with limited retrieved information. The characteristics of the conventional SAR sensor is bulky, high power, sensitive to Faraday rotation effect etc. Recently, we are developing the Circularly Polarized Synthetic Aperture Radar (CP-SAR) onboard microsatellite to retrieve the physical information of Earth surface, especially the Asian disaster area in the future.

In this research, the CP-SAR sensor is developed to radiate and receive circularly polarized wave. The sensor is designed as a low cost, simple, light, strong, low power or safe energy, low profile configuration to transmit and receive left-handed circular polarization (LHCP) and right-handed circular polarization (RHCP), where the transmission and reception are working in RHCP and RCHP+LCHP, respectively. Then these circularly polarized waves are employed to generate the axial ratio image (ARI). This sensor is not depending to the platform posture, and it is available to avoid the effect of Faraday rotation during the propagation in ionosphere. Therefore, the high precision and low noise image is expected to be obtained by the CP-SAR.

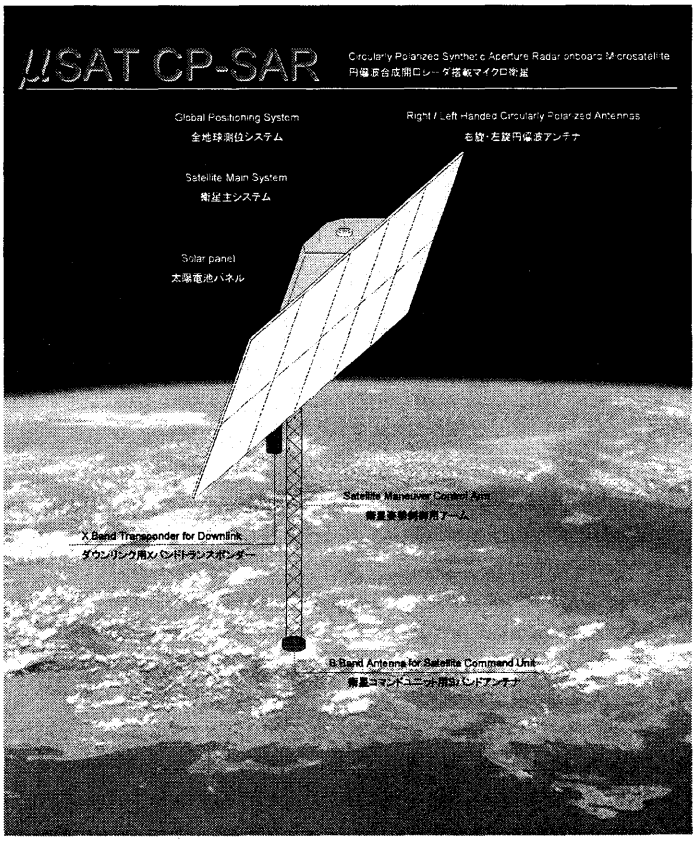


Fig. 1. Illustration of CP-SAR onboard microsatellite

The illustration of CP-SAR onboard microsatellite and its specification are shown in Fig. 1 and Table I, respectively. This satellite is composed by RCHP and LHCP antennas for CP-SAR sensor subsystem, telemetry subsystem that constructed by S band telemetry and X band transponder to transmit CP-SAR signal to ground station, and altitude controller subsystem (GPS, magnetic torque and reaction wheel assembly).

This satellite planned to be launched in 2012 with altitude between 500 km and 600 km. As shown in the specification of CP-SAR, this sensor is operated with center frequency 1.27 GHz (L band) and 10 MHz of chirp pulse bandwidth. The gain in main beam is set higher than 30 dBic to obtained received signal higher than -20 dB (equivalent backscattered noise level). The axial ratio is set lower than 3 dB to obtained ideal circular polarization. The antenna size is 1 m and 4 m for range and azimuth directions, respectively, to obtain the beamwidth 13.5° (range) and 3.4° (azimuth). The off-nadir angle is set 23°~ 35°, where the detail calculation to find this off-nadir angle will be discussed in the next Section. The transmittion antenna is RHCP, and reception is RHCP+LHCP. Fig 2 shows the developed circularly polarized antennas: (a) microstripline type, (b) microstrip type (Japan patent No. 2003-014301, International patent No. PCT/ JP03/05162, Japan patent No. 2006- 023701)

The ARI is expected to retrieve various information of Earth surface accurately and high precision. i.e. up-lift and subsidence, biomass, vegetation height and age, soil and snow physical characteristics based on the relationship between axial ratio and each characteristic. In the near future, CP-SAR is expected to improve the characteristics of conventional SAR system, especially to improve the application for disaster monitoring.

TABLE I

SPECIFICATION OF CP-SAR ONBOARD MICROSATELLITE

| Parameter | Specification |
|---|---|
| Altitude | 500 km ~ 600 km |
| Frequency $f$ | 1.27 GHz (L band) |
| Chirp bandwidth $\Delta f$ | 10 MHz |
| Polarization | Transmitter : RHCP<br>Receiver : RHCP + LHCP |
| Gain $G$ | > 30 dBic |
| Axial ratio $AR$ | < 3 dB (main beam) |
| Antenna size | 4 m (azimuth)<br>1 m (range) |
| Beam width | 3.4° (azimuth)<br>13.5° (range) |
| Ground resolution | 35.5 m |
| Swath width | 55 km |
| Off nadir angle | 23° ~ 35° |
| Power | 300 W |

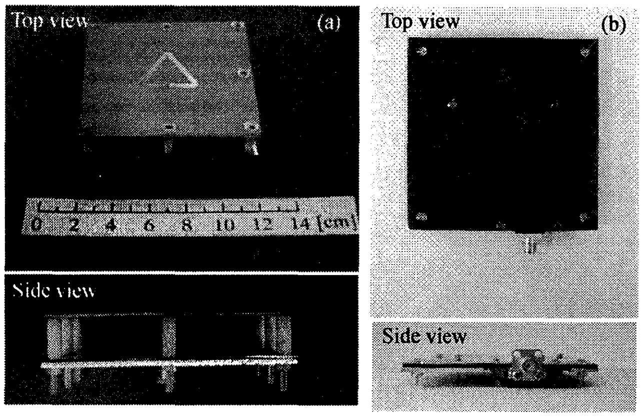


Fig. 2. Developed antennas for CP-SAR

## II. PRF CALCULATION

Base on the CP-SAR hardware specification shown in Table I, especially the antenna size, altitude (500 km to 600 km), off-nadir angle 20° to 35°, and swath width 55 km; the satisfied PRF was calculated by procedure :

(1) Minimum frequency of Pulse Repetition Frequency (PRF) is decided by Doppler bandwidth employed in azimuth compression. Here, we must consider over sampling ratio to control the azimuth ambiguity to be low.
(2) Maximum frequency of PRF is reciprocal number of total time of transmission pulse width, reception gate time and transmission-reception switching time.
(3) All scattered wave from the target in swath area must be received in reception gate.
(4) SAR sensor transmits microwave to off-nadir direction, but scattered wave from nadir (nadir echo) is very high. Therefore, nadir echo received time must be set out of reception gate time.

Base on the above conditions, the result of PRF calculation for CP-SAR sensor is obtained as below.

(1) Azimuth Doppler frequency 3,830 Hz is obtained base on azimuth antenna size. Over sampling ratio is empirically set as 1.2 to control azimuth ambiguity. Therefore, low frequency PRF is obtained about 4,600 Hz and Signal-to-Ambiguity ratio S/A at azimuth direction is obtained 22.4 dB.
(2) Maximum PRF frequency obtained 5,556 Hz by considering transmitted pulse width 30$\mu$S, reception gate 140$\mu$S to realize 21 km (slant range) swath width, transmission-reception switching time 5$\mu$S. Finally, scattered waves from observed area (swath area) are captured during reception gate time by considering minimum and maximum PRF frequencies. The results of PRF for altitude 500 km and 600 km are shown in Fig. 3.
(3) Fig. 4 shows the PRF distribution by avoiding nadir echo to be observed in reception gate time.

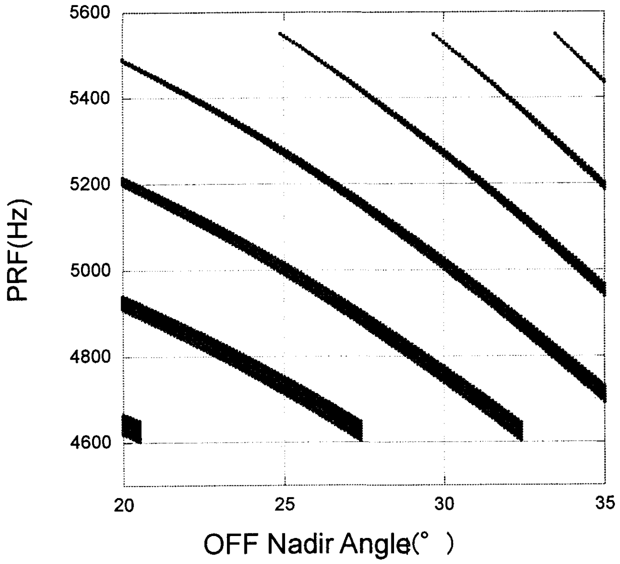


Fig. 3 (a). Satisfied PRF range (Altitude 500 km)

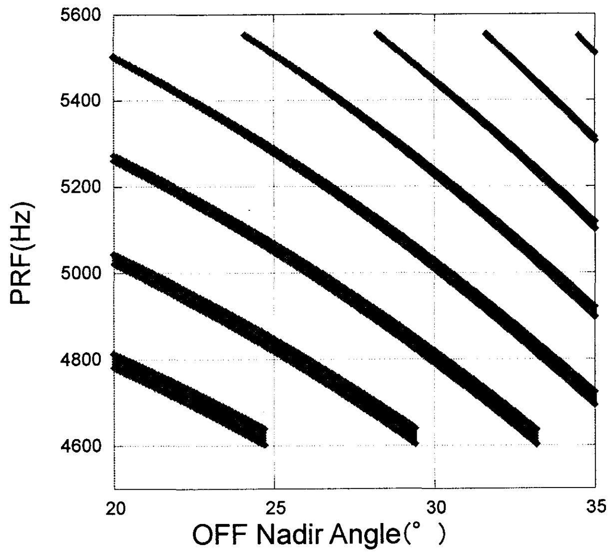


Fig. 3 (b). Satisfied PRF range (Altitude 600 km)

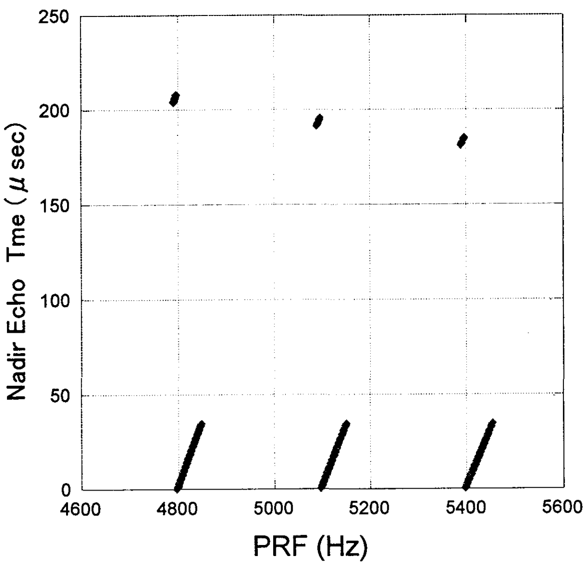


Fig. 4 (a). Nadir echo received time (altitude 500 km)

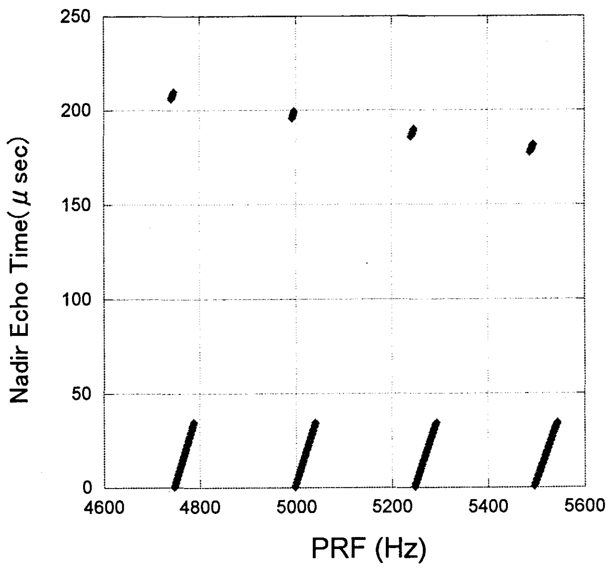


Fig. 4 (a). Nadir echo received time (altitude 600 km)

Figs. 3 and 4 show the relationship between altitude and off-nadir angle and satisfied PRF to secure the CP-SAR performance. The increasing of PRF will increase the average transmission power, data rate of CP-SAR and range ambiguity. Therefore the low PRF is must be selected to secure the CP-SAR performance. Base on Figs. 3 and 4, PRF 4,790 Hz ~ 4,850 Hz and 4,740 Hz ~ 4,790 Hz are the solutions for altitude 500 km and 600 km, respectively. Then off-nadir angle for altitude 500 km is 23°, 29° and 34°, and for altitude 600 km is 22°, 27°, 31° and 35°.

## III. CP-SAR SYSTEM

Fig. 5 shows the CP-SAR sub-system that composed by signal generator unit to generate the chirp pulse with bandwidth 10 MHz. Then this signal flows to RF circuit to be coupled -10 dB as reference signal to derive the In-phase (I) and Quadrature (Q) signal. The 300W output signal is generated by antenna controller then transmitted by right handed circular polarization (RHCP) antenna (TX). For the experiment, both RHCP and left handed circular polarization (LHCP) will be employed together, but only RHCP will be employed in microsatellite onboard CP-SAR. The reception (RX) is constructed by LHCP and RCHP antenna. The dipole antenna that working with center frequency 1.27 GHz is employed for calibration and validation.

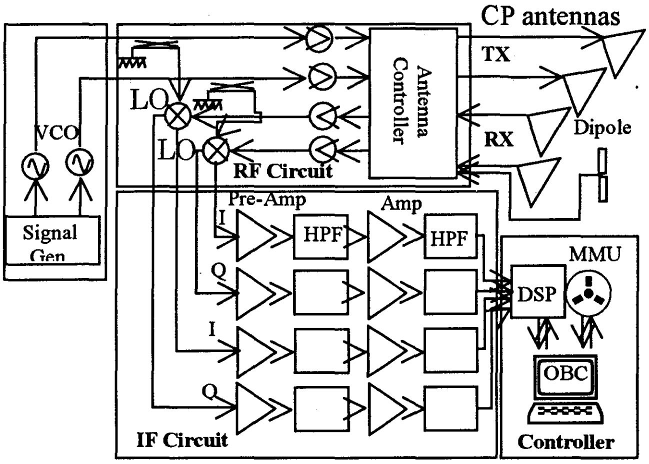


Fig. 5. CP-SAR Sub-system

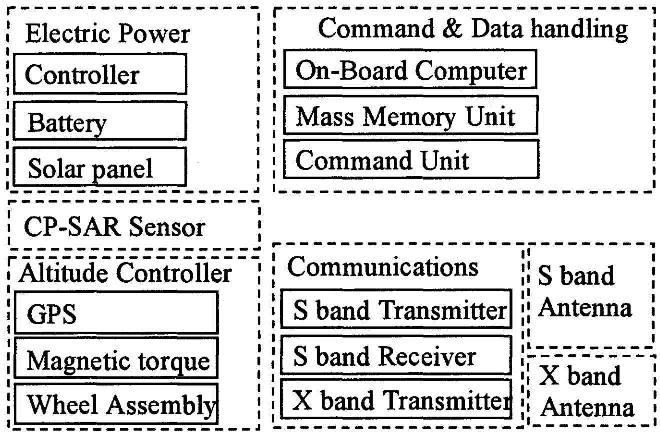


Fig. 6. CP-SAR onboard Microsatellite System

The received signal is amplified by Pre-Amp to obtain the satisfied intensity level. Then target signal is filtered by high pass filter (HPF). Then this signal is processed by DSP and On-Board Computer (OBC) in microsatellite. Temporary the signal is saved in Mass Memory Unit (MMU) before transmit to the ground station.

Fig. 6 show the CP-SAR onboard microsatellite system. This system is composed by CP-SAR sensor, electric power, altitude controller, command and data handling, and communications subsystems. Electric power subsystem supplies the electricity for CP-SAR sensor and other sub systems. In this sub system, the electricity collected by 3 $m^2$ solar panel then it charges the battery. The altitude of microsatellite is controlled by magnetic torque and wheel assembly. The information of microsatellite location is collected by GPS. This information is saved in the MMU add to the CP-SAR signal. These saved data transmit to ground station by using X band communication sub-system.Telemetry is held by using S band transmitter and receiver. Command and data handling subsystem is composed by MMU, Command Unit and On-Board Computer (OBC). The OBC is center to control the CP-SAR and other sub-systems in microsatellite. The received LHCP and RHCP signal will be processed to derive axial ratio image (ARI) to retrieve the physical information on the Earth surface. Fig. 7 shows the flow chart of CP-SAR signal processing.

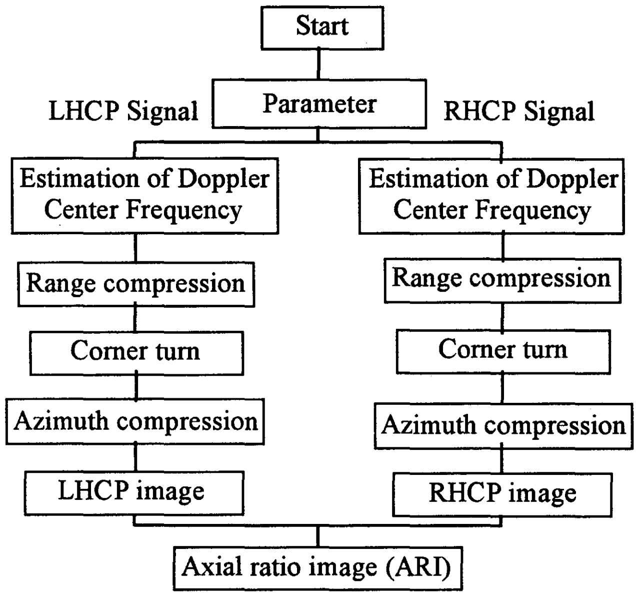


Fig. 7. CP-SAR Signal Processing flow chart

## IV. CONCLUSION

In this paper, recently our laboratory developed the Circularly Polarized Synthetic Aperture Radar (CP-SAR) onboard microsatellite to retrieve the Earth surface. This sensor is developed to monitor the disaster, especially in Asian countries, i.e. forest fire, earthquake, flood, ice berg etc. The CP-SAR sensor is developed to radiate and receive circularly polarized wave. The sensor is designed to transmit and receive left-handed circular polarization (LHCP) and right-handed circular polarization (RHCP). These circularly polarized waves are employed to generate the new type of SAR image called axial ratio image (ARI).

## REFERENCES

[1] http://www.asf.alaska.edu/reference/reference_docs.html

# Urban Sprawl Phenomenon Detection Using Spectral Mixture Analysis (SMA) from Multitemporal Landsat Satellite Images: A case study in Bandung Basin, Indonesia

Ketut WIKANTIKA[1], Ivan PRATAMA[2], Akhmad RIQQI[2], Ibnu SYABRI[3], Y. Ihya ULUMUDDIN[1], Syams NASHRRULLAH[1] and Firman HADI[1]
[1] Center for Remote Sensing, Institut Teknologi Bandung
[2] Geodetic and Geomatics Engineering, Institut Teknologi Bandung
[3]Urban and Regional Planning Engineering, Institut Teknologi Bandung
E-mail: wikantika@yahoo.com

**Abstract**
Bandung was a rapid developed city in Indonesia. However the development was unplanned and sporadic. It was urban sprawl phenomenon that was most found in developed countries. Our study was using Spectral Mixing Analysis (SMA) to detect the phenomenon using multitemporal Landsat satellite images. The most difficult process and crucial of the method was determination of end-member. The study could determine two end-member for one band of image and its were used to detect the urban sprawl phenomenon. The application of determined end-member could detect the urban sprawl and it shown that the pattern of residential land distribution is around primary road connecting Bandung and other cities around.

## 1. Introduction

Urban sprawl is defined as continues growth of urban areas, expanding to peripheral, sporadic and unplanned, and its always produce land use change from rural to urban use. The phenomenon emerges as response of spatial needs in rural for residential land, commercial and service areas, industrial areas, transportation, communication and utility land use and other public facility land use. Rapid population growth and urbanization were causes of sporadic and unplanned residential land development in rural areas. It is urban sprawl phenomenon that is found in Indonesia and other developed countries.

One of big cities that are rapidly developing in Indonesia is Bandung that has a unique magnetic power (Kompas, 2004). Bandung is one of center for mode in Indonesia. Textile and garment industries were spreading out in peripheral areas of Bandung City and it is supported by shop and store tourism for clothing and shoes. Culinary tourism is also supported the shop and store tourism. It could be unique magnetic power for tourists-most of them come from Jakarta-particularly after toll road Cikampek-Purwakarta-Padalarang corridor (connecting Jakarta and Bandung) has been opened. Not only it is making easy to access to Bandung from Jakarta, but also it could be magnetic effect for somebody, which is working in Jakarta, to live in Bandung and around. In addition, Bandung has many universities; there are three governmental universities and many non-governmental universities. Therefore many students from overall of Indonesia are interested in Bandung. All of them are making rapid urban growth in Bandung and it towards urban sprawl phenomenon.

Since 1970s, Bandung's decision-makers have known the phenomena mentioned-above. To solve the problem, Bandung and small cities around have been planned in "Bandung Raya Development" concept. But it is never being and to be far away from the concept; establishment of Cimahi City is the sign of the failure (Kompas, 2003). Unplanned urban growth is pictured on some spots such as Kopo, Setia Budhi, Ujungberung and Cimahi.

In our study will be investigated the using of multitemporal Landsat satellite images to detect width and distribution of residential land on the spots mentioned-above. Satellite images are time series data and it could be used for monitoring purposes. To achieve the aims of study, Landsat images (that has medium resolution in spatial) must be proceed by using particular methods. Thus the medium resolution satellite images could produce residential land map more accurately. Therefore Spectral Mixture Analysis will be developed in the investigation to produce the map.

## 2. Study area

The spots of residential land mentioned-above are in Bandung Basin. The areas include Bandung City, Kabupaten Bandung, Cimahi City and part of Kabupaten Garut and Sumedang. Fig. 1. is Bandung Basin map. :

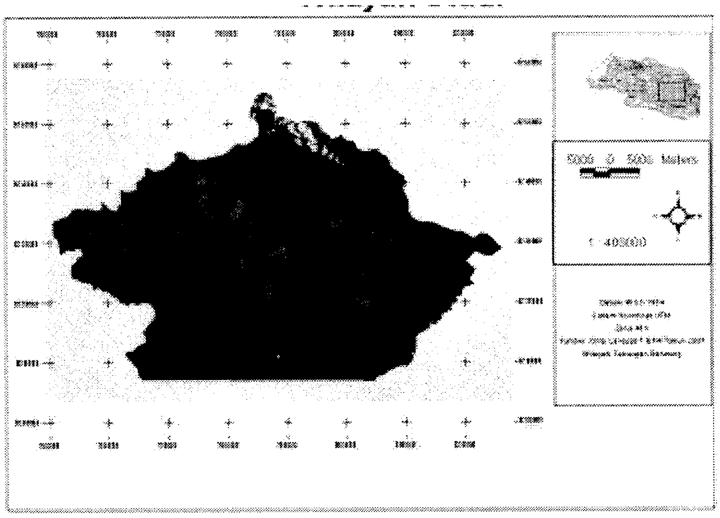

Figure 1. Bandung Basin

**3. Data and Methodology**

The study uses images of Landsat TM 1994, Landsat ETM 2001. The Landsat images are composite data, 6 bands (1-5 and 7). It is used WGS'84 for datum reference and SUTM 48 zone for projection system. The images are proceed through the stages which is shown in flowchart below:

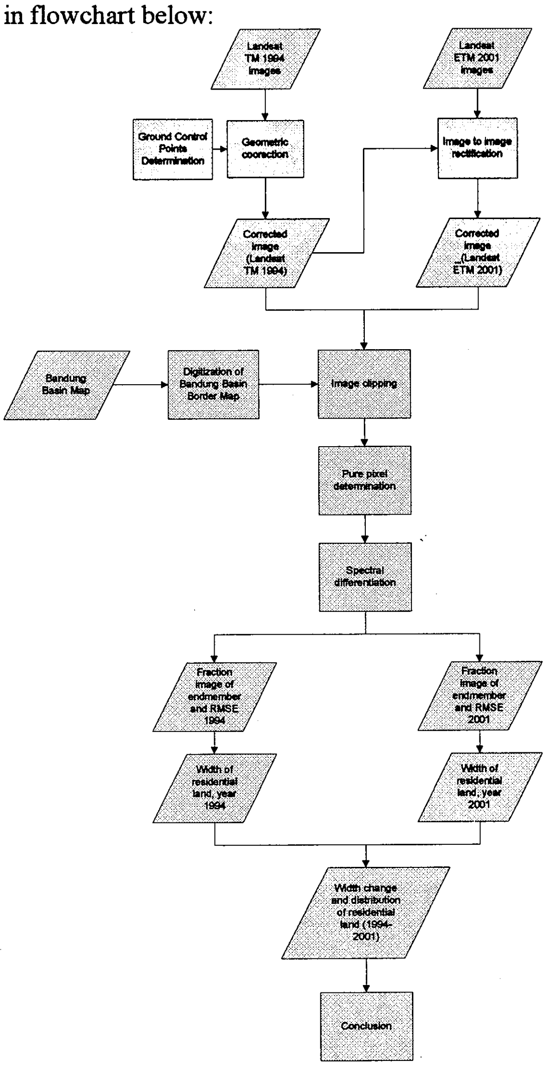


Figure 2. Flowchart of methodology

**4. Spectral Mixture Analysis**

Spectral Mixture Analysis (SMA) is a process or method to identify the different objects in one pixel of medium and low spatial resolution images. For example: Landsat and MODIS imagery respectively are 30x30 m and 250x250 m in spatial resolution. One pixel may contain more than one object, but one pixel has only one brightness value. By using SMA method, the proportion of the objects in one pixel can be identified and determined. Identified and determined the objects are defined as end-member.

The first process in SMA is determination of pure pixel. The pure pixel is pixel that contains brightness value of one object. Pure pixel determination is proceed through creating training sample end-member. The next process is calculation of each end-member fraction of images. The fraction of each end-member is inverse of matrix below (Peng and Uchida, 1999):

$$\begin{pmatrix} d_{i1} \\ d_{i2} \\ \cdots \\ d_{im} \end{pmatrix} = \begin{pmatrix} r_{11} & r_{12} & \cdots & r_{1p} \\ r_{21} & r_{22} & \cdots & r_{2p} \\ \cdots & \cdots & \cdots & \cdots \\ r_{m1} & r_{m2} & \cdots & r_{mp} \end{pmatrix} x \begin{pmatrix} f_{i1} \\ f_{i2} \\ \cdots \\ f_{ip} \end{pmatrix} \quad \cdots\cdots (1)$$

or

$$D_i = R \text{ x } f_i \quad \cdots\cdots (2)$$

where,

$d_{im}$ = brightness value of pixel $i$ and band $m$
$r_{mp}$ = brightness value of end-member $p$ and band m.
$f_{ip}$ = fraction of end-member $p$ and pixel $i$
$n$ = pixel total of overall image

with requirements:

$f_{ik} \geq 0$ , and
$f_{i1} + f_{i2} + f_{i3} + \ldots + f_{ik} = 1, \quad where\ i = 1, 2, 3, \ldots, n$ ................................(3)
and requirements of matrix to make its inverse matrix.

**5. The Result of Spectral Mixture Analysis Application**

According to the requirement of spectral differentiation matrix in eq (1), it was chose three cases for end-member determination, two end-member one band, three end-members two bands, and four end-members three bands. From three cases, two end-members one band was selected to detect residential land change in width and urban sprawl phenomena. The end-member determination is the most crucial process because probably pixels with the same brightness value (they have the same object) have different fraction magnitude. It can produce error in interpretation to define direction and magnitude of the changes. The result of selection of the cases is used to investigated urban sprawl phenomena on some spots in Bandung Basin: Kopo, Setia Budhi, Ujungberung and Cimahi.

**5.1. *Urban Sprawl* in Kopo**

Kopo areas are passed by Jalan Kopo as primary collector road collecting transportation from and to Bandung City (Fig 3). It is connecting Bandung hinterland around. It enhances the growth of residential land around Jalan Kopo (Kristiani, 2004 ).

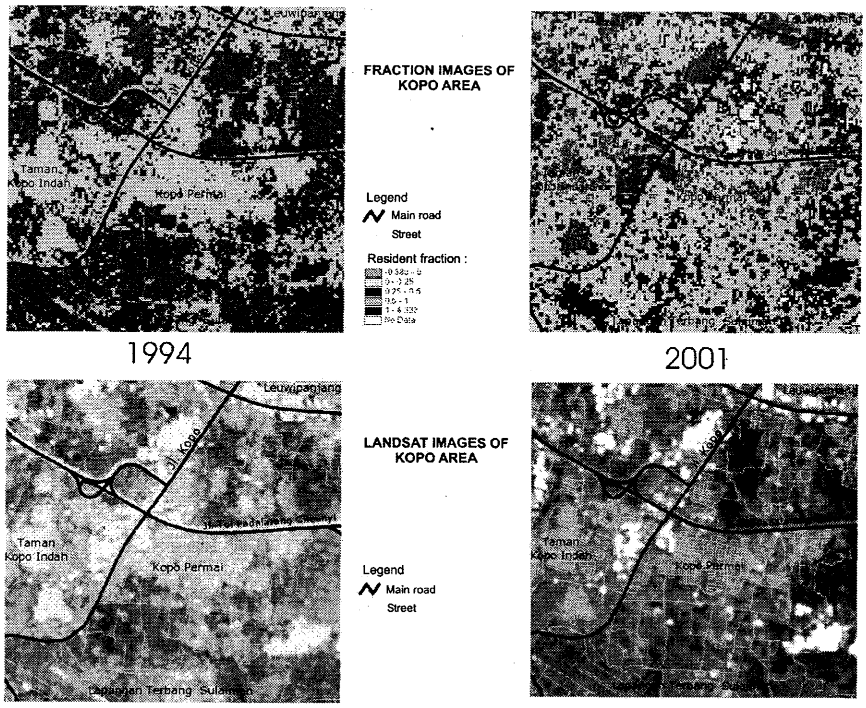


Figure 3. Fraction Images of Kopo Area

**5.2. *Urban sprawl* in Ujungberung**

Governmental Role number 16, 1987 (PP No. 16, 1987) gives a role of rural development in Bandung toward east. Unfortunately, residential land expansion is not only toward east but also toward west or center of Bandung City (Budianto, 2001). Residential land spreads out following primary road that the purpose of the road is as artery road connecting Bandung and others (Fig. 4).

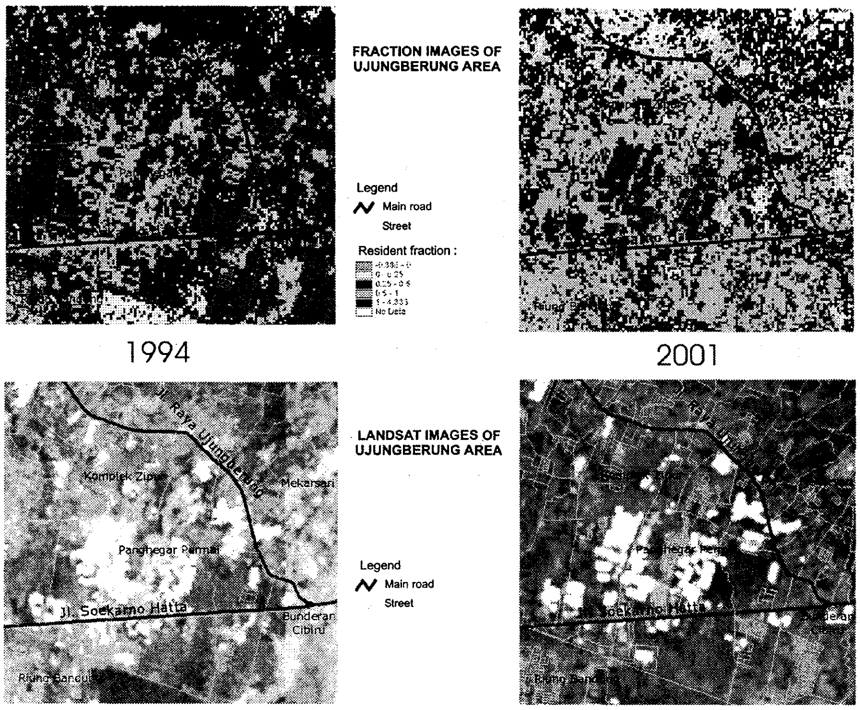


Figure 4. Fraction images of Ujungberung Area

**5.3. *Urban sprawl* in Setia Budhi**

The residential land of two spots above growths rapidly because it is supported by the road connected Bandung and others. Residential land expansion in Setia Budhi follows Jalan Setia Budhi, the easier access to governmental facilities and commercial and service facilities (Fig. 5). In addition, mountain air-fresh (ten years before) in Setia Budhi areas is one of reasons to build houses. Jalan Setia Budhi is also as primary road connected to tourism areas in Lembang and Kabupaten Subang.

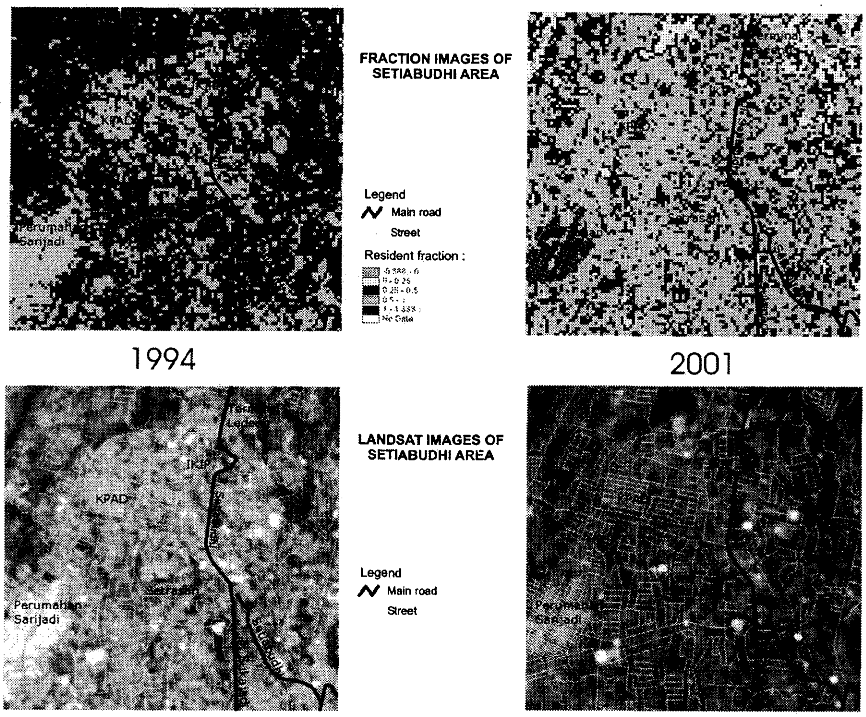


Figure 5. Fraction Images of Setia Budhi Area

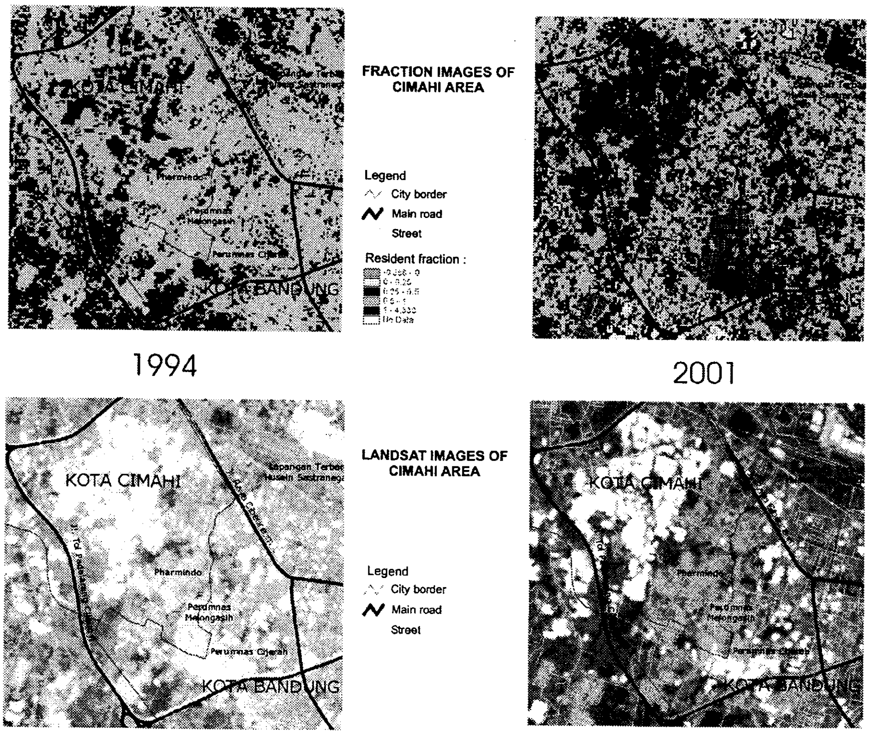


Figure 6. Fraction images of Cimahi Area

**5.4.** ***Urban sprawl* in Cimahi**

Different from three spots above, residential land expansion in Cimahi follows the rural growth as center for military training and education and industrial areas to improve the income of Kabupaten Bandung (before being Kota Cimahi). Residential land growth in the spot overlaps with the two activities. Population growth in Cimahi enhances development of commercial and service areas that its placement also overlaps with other land use. The development is enhanced by strategic position as a gate of Bandung City in the south (Fig. 6).

## 6. Conclusion

The use of Spectral Mixture Analysis method has difficulties on end-member determination. From three cases end-member determination, two end-members, one band was selected to detect residential land growth in Bandung Basin. In general, residential land growth on the spots investigated follows road development, particularly the roads connected to other city.

## References


Budianto, F. 2001. Karakteristik Perjalanan Penghuni Perumahan Formal dan Pengaruhnya Terhadap Tingkat Pelayanan Jalan Raya Timur Bandung. Kasus Perumahan Formal di Kawasan Ujungberung Bandung. Departmen Teknik Planologi. Institut Teknologi Bandung. Bandung. Indonesia

Kristiani, L.A. 2004 Kajian Perubahan Tingkat Pelayanan Jalan Kopo Bandung dengan Pengelolaan Lalu Lintas. Skripsi. Departemen Teknik Planologi. Institut Teknologi Bandung. Bandung. Indonesia

Layuck, J. R. 2003. ________________. Kompas, 30 November 2003. Jakarta. Indonesia

Suganda, H. 2004. Bandung Raya, Apakah masih relevan?. Kompas, 6 Desember 2004. Jakarta. Indonesia.

Peng, Y and Uchidas. S. *The Use of Linear Spectral Unmixing Model for Improving Estimation Accuracy of Winter Wheat Acreage – A Case Study in Shunyi County*. Beijing. China.